Optimization of power conversion efficiency of $CH_3NH_3PbI_3$ perovskite solar cell with TiO_2 as electron transport layer

F. Otmani [a,*], N. Bachir [a], A. Merad [b]
[a] *Unity of Research of Materials and Renewable Energies (URMER)*
[b] *Theoretical Physics Laboratory University of Tlemcen BP: 119 Tlemcen 13000 Algeria*

Because of its interesting optoelectronic properties, Methylammonium Lead Iodide $CH_3NH_3PbI_3$ perovskite semiconductor is used as an active layer in the development of several emerged solar cells. In this work, the solar cell with the architecture FTO/TiO_2/ $CH_3NH_3PbI_3$/Spiro-MeOTAD/Au is simulated using the sophisticated OghmaNano software. We have studied the influence of some parameters like thickness for different layers, charge carrier mobility of holes and electrons, charge recombination rate, band gap energy and doping in the active layer. The effect of device temperature is also studied. The photovoltaic characteristic curves such as Current density-Voltage (J-V), is represented in this work. The final optimized parameters Jsc, Voc, FF and PCE are 34.14 mA/cm^2, 0.95 Volt, 82.28 % and 26.13 % respectively.

(Received November 4, 2024; Accepted February 5, 2025)

Keywords: OghmaNano software, Perovskites Solar Cell, $CH_3NH_3PbI_3$, Conversion efficiency.

1. Introduction

The Perovskite based represent origin of many researches in the field of physics, in particular in the development of solar energies. Cells are innovative photovoltaic devices that use perovskite-based materials to convert solar light into electricity. Perovskites were first discovered by G. Rose in 1839. They are characterized by their different crystalline structure consisting of metal cations at the center surrounded by anions. This specific crystalline structure gives them interesting properties such as electrical conductivity, thermal conductivity, photoluminescence, and light absorption. They are also known for their flexibility and ability to be chemically modified to obtain specific properties. This allows them to have applications in various fields of materials science.

Also, because of its direct gap which varies between 1.66 eV and 1.55 eV [1], the perovskite Methyl ammonium lead iodide, $CH_3NH_3PbI_3$, is a semiconductor material contains interesting optical and electronic properties. It has an important absorption coefficient. Electrons and holes, have high mobility in this material. The efficiency of the perovskite solar cells using $CH_3NH_3PbI_3$ has evolved between 3.8% in 2009 [2] and 25.03% in 2023 [3], and it is limited to 31% [4]. Because their low production price and high efficiency perovskite solar represents a good choice in commerce of photovoltaic field.

Our sandwich is made up of a first layer Fluorine-doped Tin Oxide (FTO) which is used as a transparent conductive layer (TCO) to allow light to enter the cell. The second layer is Titanium oxide (TiO_2) to facilitate electron transport as an Electron Transport Layer (ETL); the third material is the perovskite Methyl ammonium lead iodide $CH_3NH_3PbI_3$ as an active layer a spiro-MeOTAD which is an organic material used as the hole transport layer (HTL) in perovskite solar cells. It is transparent in the visible range, stable and has good electrical performance, making it a popular choice for improving the performance of solar cells. Finally, the electrons are collected using a (Au) as metal layer.

* Corresponding author : fz_otmani@yahoo.com
https://doi.org/10.15251/JOR.2025.211.95

Firstly, we have varied the thicknesses of the different active layers in order to optimize the solar cell structure. and secondly, we have studied the influence of different parameters such as charge carrier mobility of holes and electrons, charge recombination rate, band gap energy and doping in the active layer and the effect of temperature on the characteristics of perovskite solar cells, and finally for the optimization of the optical characteristics we have launched an optical simulation using the OghmaNano software.

2. Simulations model

OghmaNano is a free general-purpose tool for photovoltaic device Simulation based on solving Poisson equation (eqs. 1) to calculate the internal electrostatic potential. Both electrons and holes drift-diffusion (eqs.2,3), The model can describe a Recombination and carrier trapping by using Shockley-Read-Hall (SRH) formalism, the distribution of trap sates can be also defined (4,5) given as below:

$$\frac{d}{dx}\varepsilon_0\varepsilon_r = \frac{\partial\varphi}{\partial x} = q(n-p) \tag{1}$$

$$J_n = q\mu_c n\frac{\partial E_c}{\partial x} + qD_n\frac{\partial n}{\partial x} \tag{2}$$

$$J_p = q\mu_n p\frac{\partial E_v}{\partial x} + qD_p\frac{\partial p}{\partial x} \tag{3}$$

$$\frac{\partial J_n}{\partial x} = q\left(R_n - G + \frac{\partial p}{\partial x}\right) \tag{4}$$

$$\frac{\partial J_p}{\partial x} = -q\left(R_n - G + \frac{\partial p}{\partial x}\right) \tag{5}$$

The fundamental electrical parameters of solar can be analyzed by examining the current-voltage curve. We can also cite: short circuit current (Isc), open- circuit voltage (Voc) (6), fill factor (FF) (7) and power conversion efficiency (PCE) (8) [5].

$$v_{oc} = \frac{q}{nKT}V_{oc} \tag{6}$$

$$FF = \frac{v_{oc} - ln(v_{oc}+0.73)}{v_{oc}+1} \tag{7}$$

$$PCE = FF\frac{I_{SC}v_{oc}}{P_{IN}} \tag{8}$$

In Figure 1, is represented the architecture of the heterojunction $CH_3NH_3PbI_3$ based solar cell. The layer configuration assumed in this simulation is (FTO/TiO_2/$CH_3NH_3PbI_3$/Spiro-MeOTAD/Au). The physical parameters of active layer used for the simulation are depicted in Table 1.

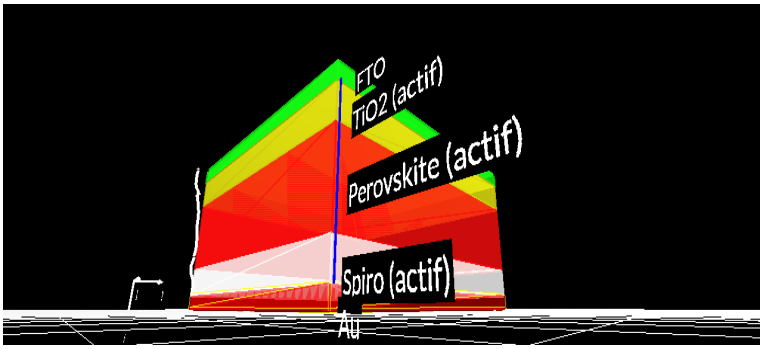

Fig. 1. Planar hetero junction structure of a typical perovskite solar cell.

Table 1. Physical parameters of active layer used for the simulation.

Parameters	Values
Layer thickness (m)	variable
Band gap (eV)	1.6
Electron affinity (eV)	3.7
Electron mobility (m^2 /V.s)	0.002
Hole mobility (m^2 /V.s)	0.002
Effective density of free electron states (m^{-3})	10^{26}
Effective density of free hole states (m^{-3})	10^{26}
Electron tail slope (eV)	0.06
Hole tail slope (eV)	0.06
Relative permittivity (au)	20.0
Electron trap density (m^{-3} eV^{-3})	10^{20}
Hole trap density (m^{-3} eV^{-3})	10^{20}
Free electron to trapped electron (m^{-2})	10^{-20}
Free hole to trapped hole (m^{-2})	10^{-20}
Trapped electron to free hole (m^{-2})	10^{-22}
Trapped hole to free electron (m^{-2})	10^{-22}
Number of traps bands	5

3. Results and discussion

Our first simulation is based on the variation of the thickness of the different layers ($CH_3NH_3PbI_3$, FTO, TiO_2 and Spiro-MeOTAD) to have the best power conversion efficiency PCE. Then, we have studied the influence of some parameters like charge carrier mobility of holes and electrons, charge recombination rate, band gap energy and doping for the active layer on different characteristics of solar cells (PCE, FF, Jsc and Voc). Finally, the effect of temperature is also studied.

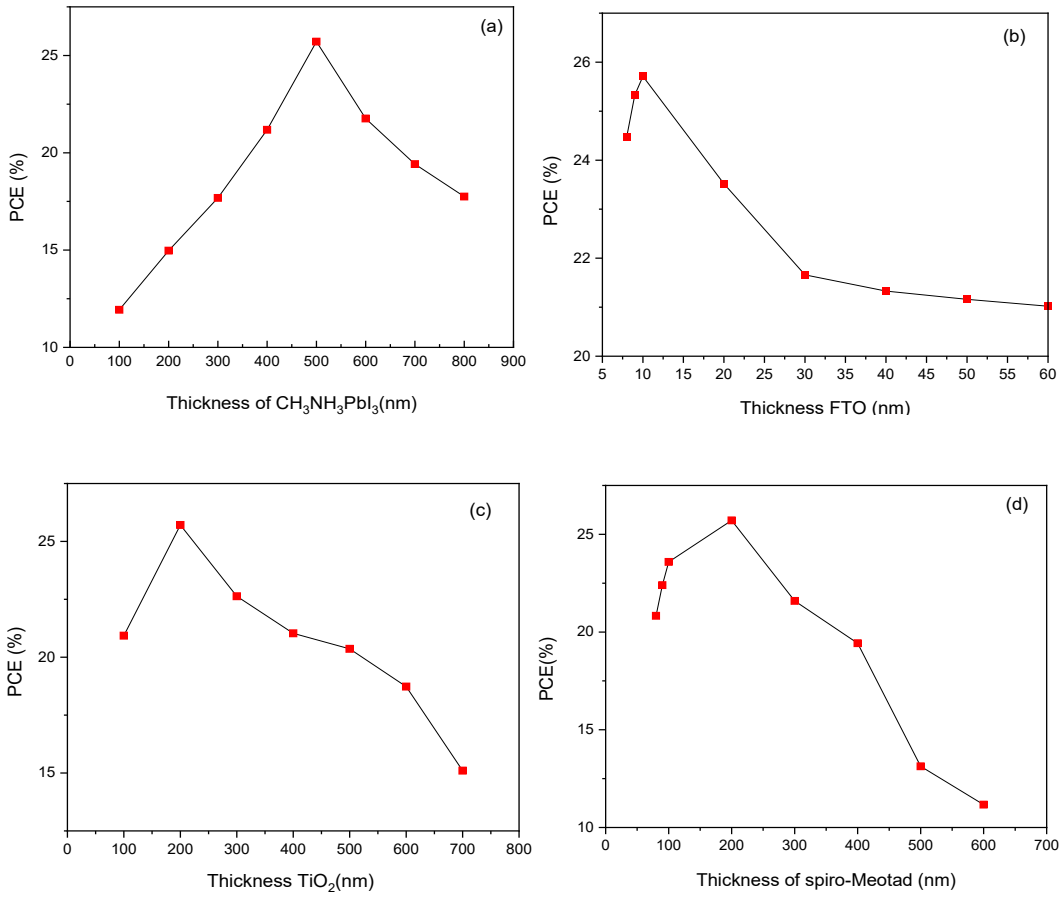

Fig. 2. PCE as function of the layers thickness of: a) $CH_3NH_3PbI_3$, b) FTO, c) TiO_2 and d) spiro-MeOTAD.

Figure 2.a shows that the PCE increases with the increase of the $CH_3NH_3PbI_3$ absorber layer thickness until reaching the maximum value of 25.71% at 500 nm and decreases after that. The associated parameters: Jsc, Voc and FF increase too. The percentage of absorbed light increases with the increase in thickness of the $CH_3NH_3PbI_3$ absorbing layer. Therefore, Jsc increases, then, it decreases with increasing thickness of the absorbing layer due to the limited penetration of incident light AM 1.5 G light. The FTO layer eliminates the charge recombination process and the use of TiO_2, assuring the electron collection procedure [6]. The effect of TiO_2 and FTO layer thickness in PCE is represented in Figure 2.b and 2.c. The PCE reached 25.71% until 200nm for TiO_2 and 10nm m for FTO than decreases with further increase in thickness. This is due to the higher recombination of charges. The maximum value of Voc is 0.94 V which is reached with an absorber layer thickness of 500nm. Voc decreases with increasing thickness of the $CH_3NH_3PbI_3$ absorber, this is result to increased recombination in the absorber due to the short lifetime of the charge carriers. Also increasing the thickness of the absorbent layer leads to a reduction in the effective band gap, which in turn leads to a reduction in Voc. Figure 2.d shows that the best PCE is obtained for 200nm for spiro-MeOTAD thickness layer, a thick layer of spiro-MeOTAD increases series resistance, reducing fill factor (FF) and efficiency.

In this part, we studied the effect of charge carrier mobility of holes and electrons in the active layer on the different electrical characteristics of our cell such as current density (Jsc), full factor (FF), open- circuit voltage (Voc) and conversion efficiency (PCE). We have varied the mobility from 2×10^{-7} m^2/Vs to 2×10^{-1} m^2/Vs. The results of the simulation are reported in the table 2 and fig.3. (a, b).

Table 2. Solar cell parameters for different mobility

Mobility (m^2/VS)	J_{SC} (mA/cm^2)	V_{oc}(volt)	FF (%)	PCE (%)
2× 10^{-7}	09.410	0.9736	27.3	02.50
2× 10^{-6}	15.510	0.9837	47.51	07.30
2× 10^{-5}	32.410	0.9811	59.94	19.06
2× 10^{-4}	34.020	0.9491	74.19	23.93
2× 10^{-3}	34.024	0.9400	79.52	25.44
2× 10^{-2}	34.114	0.8812	81.21	24.42
2× 10^{-1}	34.201	0.8419	79.27	22.83

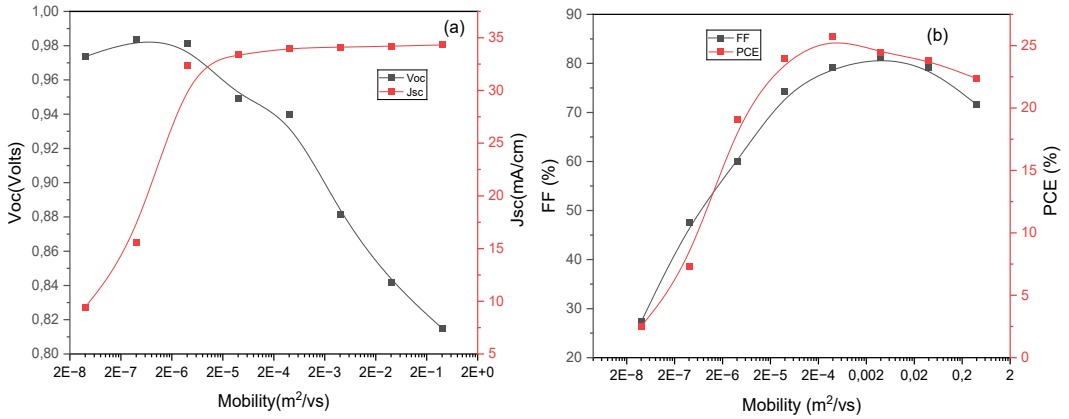

Fig. 3. (a, b). Effect of mobility on a) Open-circuit voltage, short-circuits current density b) Conversion efficiency, and fill factor.

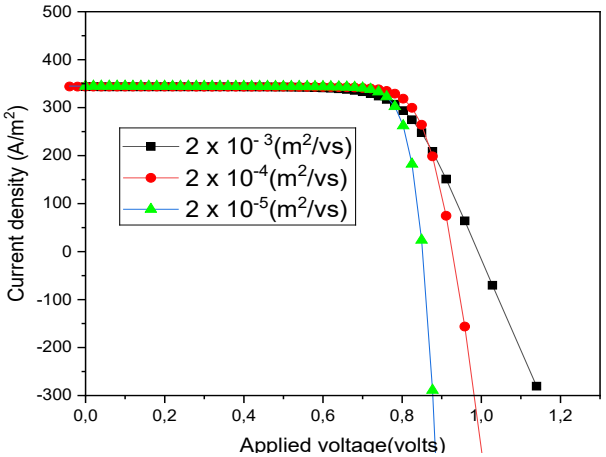

Fig. 4. Current density-voltage (J-V) for different mobility.

The mobility of charge carrier is a responsible element of the two opposing processes, recombination and extraction charge carrier in the solar cell. Increased mobility of charge carriers would improve extraction, but would also increase recombination charge, which would have a beneficial influence on charge carrier transport. The current density increases as mobility carrier increases which results in high full factor and efficiency. Due to the probability of separation and bed transport of charge carriers as carrier mobility decreases the current density decreases. The open-circuit voltage drops as carrier transport improves due to increasing internal power depletion, reducing the influence of an embedded electric field. The PCE conversion efficiency varies from

25.44% to 2.5% and presents a maximum at the mobility of 2.10^{-3} $m^2/v.s$ which results in the increase in the current density. The same behavior is valuable also for FF, because it is inversely proportional to the open circuit voltage Voc. Fig.4 shows The JV characteristic for different mobility.

This section is reserved for studying the effect of charge recombination rate on the characteristics of the dispositive. Table (3), fig.5(a, b) show the variation of open circuit voltage Voc, fill factor FF, current density J_{SC} and efficiency PCE as a function of charge recombination rate. We can note that the four parameters are at a maximum at a recombination rate equal to 10^{-15} m^3/s and then have a considerable drop when the recombination rate increases. The increase in the rate of recombination will give the charges a chance to recombine before they reach the electrodes, which greatly affects the efficiency of the photovoltaic cell.

Table 3. Solar cell parameters for different charge recombination rate.

Charge recombination rate (m^3/s)	J_{SC} (mA/cm^2)	V_{oc}(volt)	FF (%)	PCE (%)
10^{-10}	24.68	0.7410	73.05	12.90
10^{-11}	32.35	0.8007	74.60	19.32
10^{-12}	34.15	0.8582	78.87	23.12
10^{-13}	34.36	0.9039	80.64	25.05
10^{-15}	34.38	0.9450	79.15	25.71

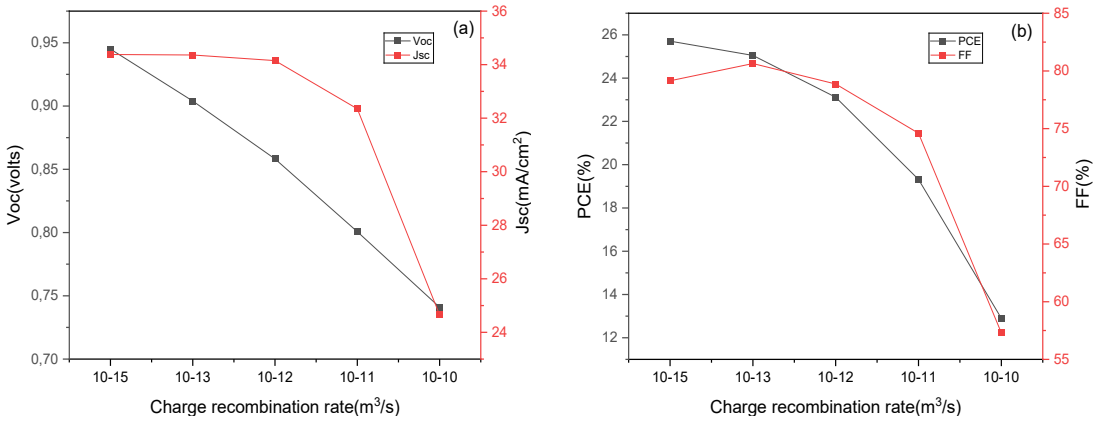

Fig. 5. (a, b). The variation of a) Open-circuit voltage, short-circuits current density b) Conversion efficiency, and fill factor as a function of charge recombination rate.

The effect of the perovskite band gap energy on the PCE, fill factor, short-circuit current density and open-circuit voltage were studied in this part and represented on table 4 and fig.6 (a, b) respectively .In this simulation, we have varied the band gap (BG) of the perovskite from 1.55 eV to 1.6 e V, We can see from the simulation results that BG variation increases PCE, FF and Voc reaching its maximum in 1.6 eV, but it has no effect on short-circuit current density. Also, the current density - voltage (J-V) for different $CH_3NH_3PbI_3$ band gap is represented in fig.7. As conclusion we can say that BG modulation is a very important parameter in perovskite cell engineering, and its role greatly influences the efficiency of the solar cell efficiency.

Table 4. Solar cell parameters for different $CH_3NH_3PbI_3$ band gap.

Band gap (eV)	J_{SC} (mA/cm^2)	V_{oc}(volt)	FF (%)	PCE (%)
1.55	34.38	0.8354	78.84	22.64
1.56	34.38	0.8820	80.91	24.54
1.57	34.38	0.8904	81.34	24.90
1.58	34.38	0.9000	81.49	25.24
1.59	34.38	0.9087	81.75	25.53
1.60	34.38	0.9120	82.01	25.71

The following section is reserved for studying the effect of doping on the various parameters of our structure, as shown on table 5 and fig.8 (a, b). We notice that PCE, Jsc and FF remain stable up to 10^{18} cm^{-3} then gradually decrease when Nd increase, this is possible due to the increased recombination rate of charge carriers and reduced charge mobility inside the perovskite absorbing layer.

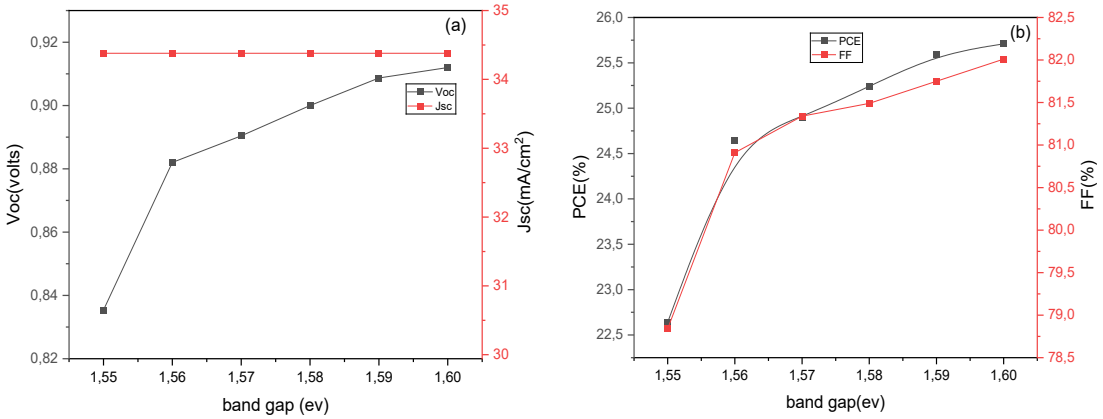

Fig. 6. (a, b). The variation of a) Open-circuit voltage, short-circuits current density b) Conversion efficiency, and fill factor as a function of $CH_3NH_3PbI_3$ band gap.

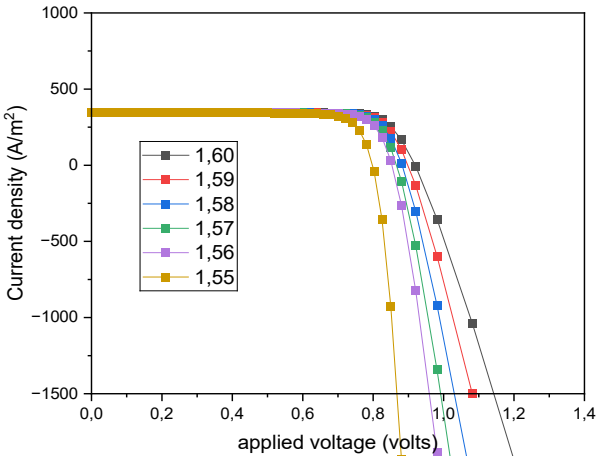

Fig. 7. Current density – voltage (J-V) for different $CH_3NH_3PbI_3$ band gap.

Doping introduces additional charge carriers into the active layer, which corresponds to the density of charge carriers (electrons or holes). Accumulated carrier density can lead to improved charge separation and reduced recombination, which increases quasi-Fermi level separation, essential for high Voc. We conclude that increasing the doping value reduces the photovoltaic performance of the cell. Our choice is fixed on the value 10^{18} cm^{-3} for better performance.

Table 5. Solar cell parameters for different $CH_3NH_3PbI_3$ doping variation (Nd).

Nd (cm^{-3})	J_{SC} (mA/cm^2)	V_{oc}(volt)	FF (%)	PCE (%)
10^{10}	34.14	0.9553	82.28	26.13
10^{11}	34.14	0.9553	82.28	26.13
10^{12}	34.14	0.9553	82.28	26.13
10^{13}	34.14	0.9553	82.28	26.13
10^{14}	34.14	0.9553	82.28	26.13
10^{15}	34.14	0.9553	82.28	26.13
10^{16}	34.14	0.9553	82.28	26.13
10^{17}	34.14	0.9553	82.28	26.13
10^{18}	34.14	0.9553	82.28	26.13
10^{19}	34.13	0.9554	80.07	26.11
10^{20}	34.09	0.9564	79.56	25.94
10^{21}	33.10	0.9628	74.48	23.73
10^{22}	21.82	0.9859	70.36	16.64
10^{23}	14.70	1.0050	68.90	12.26

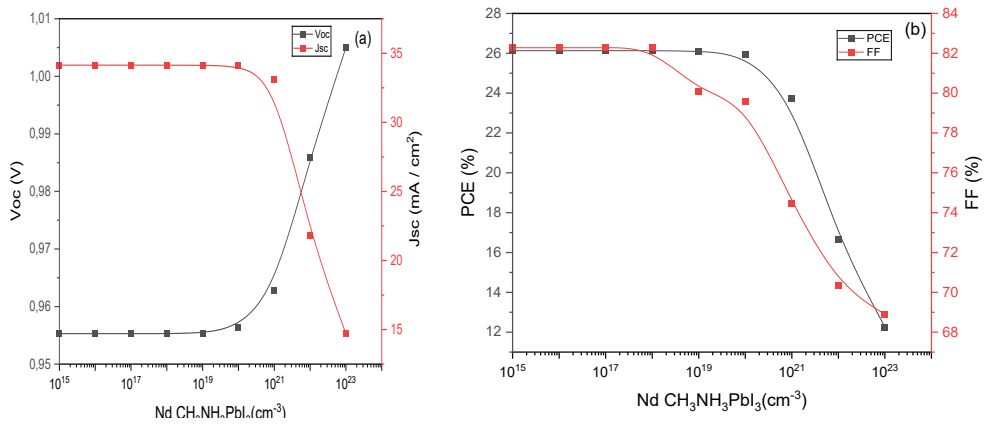

3Fig. 8. (a, b). The variation of a) Open-circuit voltage, short-circuits current density b) Conversion efficiency, and fill factor as a function of $CH_3NH_3PbI_3$ doping (Nd).

The table 6 and fig.9 show the influence of electrode nature on different device characteristics. We observe that the different characteristics are very close but the best results are obtained with Au. In addition, we observe that Al and Ag are very competitive to Au and economically are shipper.

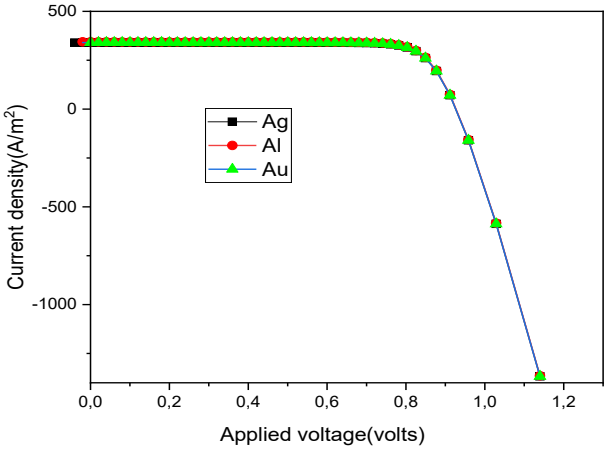

Fig. 9. Current density – voltage (J-V) for different electrode.

Table 6. Effect of different electrode on the Device performance parameters.

	J_{SC} (mA/cm^2)	V_{oc}(volt)	FF (%)	PCE (%)
Au	34.38	0.9450	79 .11	25.71
Al	34.02	0.9449	78.13	25.441
Ag	34.02	0.9449	78.15	25.442

Voc strongly depends on temperature, as shown in Fig.10.a, it decreases with increasing temperature due to change in entropy, and electron-hole pairs minimize the electrochemical energy in the conduction and valence bands, which leads to a broadening of the Fermi-Dirac distribution [7]. Fig.10.b shows the temperature dependence of PCE and FF, it is evident that the series resistance increases at high temperature, so the recombination rate also increases and the carrier diffusion length decreases. Therefore, FF decreases due to the relation that exists between FF and the series resistance (equation 9). Finally, it is evident that PCE decreases with increase in temperature because of the decrease of Voc and FF but it has no effect on short-circuit current density.

The penultimate simulation shows the effect of temperature on Solar cell parameters as indicated table 7 and fig.10 (a, b).

Table 7. Solar cell parameters for different device temperature.

Temperature (K)	J_{SC} (mA/cm^2)	V_{oc}(volt)	FF (%)	PCE (%)
300	34.38	0.94	79.75	25.71
310	34.38	0.9035	79.11	24.57
320	34.39	0.8808	78.55	23.79
330	34.39	0.8571	78.15	23.03
340	34.39	0.8331	77.63	22.24
350	34.39	0.8095	76.90	21.41
360	34.39	0.7862	76.06	20.57
370	34.39	0.7632	75.11	19.71

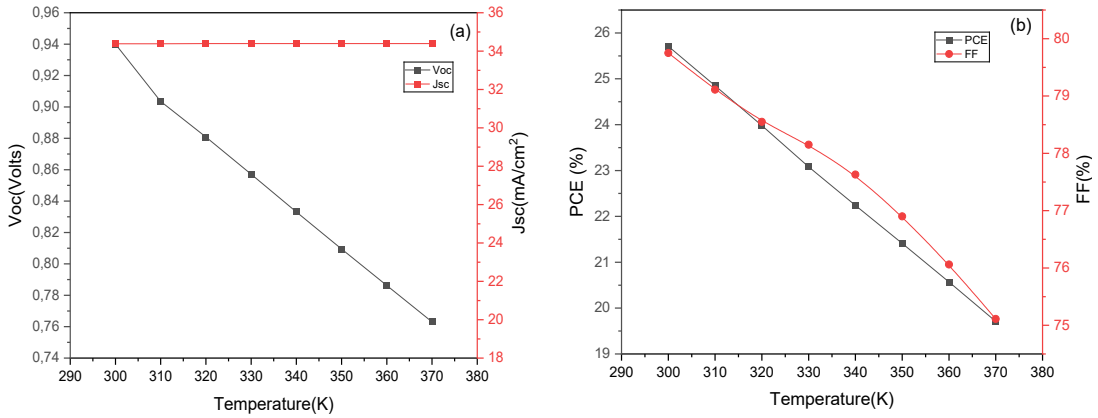

Fig. 10. (a, b). The variation of a) Open-circuit voltage, short-circuits current density b) Conversion efficiency, and fill factor as a function temperature.

$$FF \approx \left(1 - \frac{R_S I_{sc}}{V_{oc}}\right) \tag{9}$$

Due to their direct band gap and high optical absorption coefficient, $CH_3NH_3PbI_3$ perovskite absorbs sufficient solar energy which leads to a high efficiency value, consequently the external quantum efficiency EQE(fig.11) covers a wide range going from ultraviolet, where the photons in UV contribute to the generation of the photocurrent, in the visible spectrum, it reaches the maximum at 480 nm due to the strong reflection of FTO substrates at these wavelengths; and can cover even the near infrared.

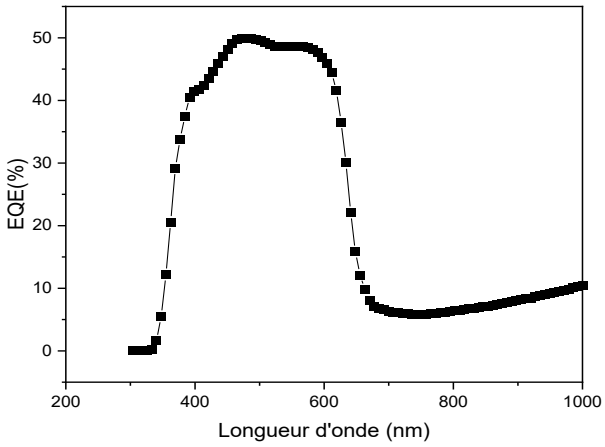

Fig. 11. EQE spectra of FTO/TiO2/ $CH_3NH_3PbI_3$/ Spiro-MeOTAD /Au structures.

After the simulation of various parameters, we obtained the best performance model FTO (10nm)/Tio_2 (200 nm) /$CH_3NH_3PbI_3$ (500nm)/ Spiro-MeOTAD (200nm)/ Au (100nm) with PCE of 26.13%. The obtained optimum parameters Voc, Jsc, and FF of the solar cell are 0.95 V, 34.14 mA/cm^2 and 82.28% respectively. For charge carrier mobility of holes and electrons, charge recombination rate, band gap energy and doping we choose 2.10^{-3} m^2/Vs, 10^{-15} m^3/s,1.6 eV and 10^{18}cm^{-3} respectively. Current density -voltage (J-V); characteristics of the optimized and initial structure are showed in the Fig.12 obtained at 300 K; at this temperature, perovskite exhibits a tetragonal phase [8], which contribute to maximum efficiency [9–10-11]; due to favorable band alignment, reduced defect densities and charge transport properties.

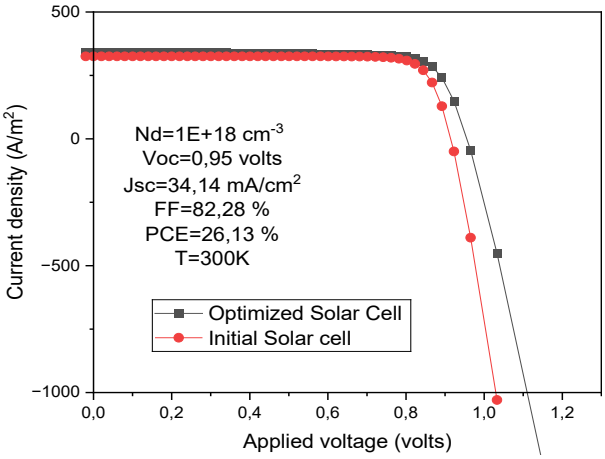

Fig. 12. Current density – voltage (J-V) for optimized and initial cells.

Table 8 shows a comparison of the electrical parameters found in our study with others works.

Table 8. Comparison of proposed model with literature.

Charge recombination rate (m^3/s)	J_{SC} (mA/cm^2)	V_{oc} (volt)	FF (%)	PCE (%)
[8] SiO_2/FTO/$CH_3NH_3PbI_3$/SpiroMeOTAD/Ag	39.15	0.90	83.58	25.59
[12] ITO/PEDOT:PSS/$CH_3NH_3PbI_3$/ZnO/Al	29.21	1.005	88.00	25.75
[7]FTO/TiO_2/ZnO/C_{60}/ $CH_3NH_3PbI_3$/V_2O_3/ Pedot:PSS/Ag	39.60	0.950	83.50	31.40
Our results	34.14	0.95	82.28	26.13

Optical simulation by ogma has various tabs that can be used to explore how light interacts with the device. Using the optical simulation technique by OghmaNano software from AM 1. 5G solar energy, we obtained the spectral distribution of incident photons and the absorbed photons in the device fig.13 and fig.14 respectively, where we can view the photon density and the rate of photon absorption in the device and describe the energy band gap of different layers [13-14]. We can also shoot the Photon efficiency, this parameter gives how many electron-hole pairs each photon that is absorbed within the active layer generates, in our device it is order of 0.6. More detail on optical simulation by OghmaNano is given in the literature [15-16].

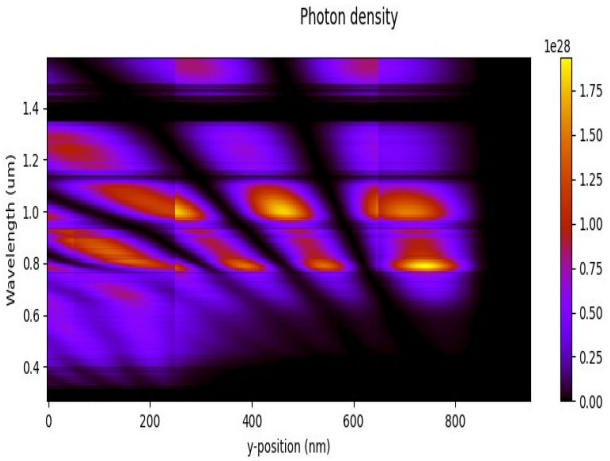

Fig. 13. Spectral distributions of incident photons.

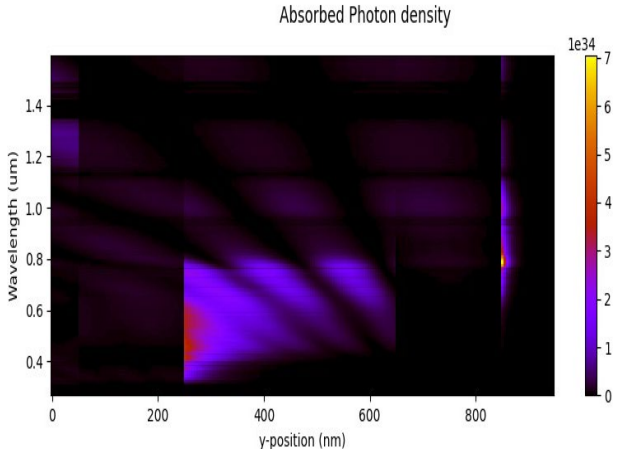

Fig. 14. Spectral distributions of absorbed photons.

4. Conclusion

The power conversion efficiency of perovskite solar cells was analyzed using OghmaNano software simulation. We found that tuning the thickness of the active layer from 100nm to 800m changed the device performance. Maximum efficiency was achieved for perovskite $CH_3NH_3PbI_3$ (500nm), FTO (10nm), TiO_2 (200nm), Spiro-MeOTAD (200nm) and Au (100nm). The effect of device temperature was also investigated and the optimum operating temperature was found to be 300K. The obtained optimum parameters Voc, Jsc, FF and PCE of the device are 0.95 V, 34.14 mA/cm^2 and 82.28% and 26.13 % respectively.

As a perspective, we will study the characteristics and electrical properties of the perovskite/Si tandem structure to improve the efficiency of perovskite based solar cells.

Nomenclature

ε_0: the permittivity of free space
ε_r: the relative permittivity
φ: the voltage profile
q: the elementary charge on an electron
n: the free electron concentration
p: the free hole concentration
Jn: the electron current flux density
Jp: the hole flux density
μ_c: the electron mobility
μ_h: the hole mobility
Dn: the electron diffusion coefficient
Dp: the hole diffusion coefficient
Rn: the net recombination rate for electrons
Rp: the net recombination rate for holes
G: the free carrier generation rate
Pin: incident power.
PCE: power conversion efficiency.
FF: fill factor variation
Jsc: the Current density.
Voc: Open circuit voltage.
R_S: the series resistance.

References

[1] T. Baikie, Y. Fang, J. M. Kadro, M. Schreyer, F. Wei, S. G. Mhaisalkar, M. Graetzel, T. J. White, Journal of Materials Chemistry A, 1(18): 5628-5641 (2013); https://doi.org/10.1039/c3ta10518k

[2] Akihiro Kojima, KenjiroTeshima, YasuoShirai, Tsutomu Miyasaka, Journal of the American Chemical Society, 131(17): 6050-605 (2009); https://doi.org/10.1021/ja809598r

[3] H. Su, Z. Xu, X. He, Y. Yao, X. Zheng, Y. She, Y. Zhu, J. Zhang, S. Liu, Adv. Mater. 36 (2) 2306724 (2024); https://doi.org/10.1002/adma.202306724

[4] Wei E. I. Sha, Xingang Ren, Luzhou Chen, Wallace C. H. Choy, Applied Physics Letters, 106(22): 221104 (2015); https://doi.org/10.1063/1.4922150

[5] Green M. A., Solid-State Electronics, 24(8): 788-789 (1981); https://doi.org/10.1016/0038-1101(81)90062-9

[6] Yang G, Tao H, Qin P, Ke. W, Fang G J. Mater. Chem. A 4 3970(2016); https://doi.org/10.1039/C5TA09011C

[7] Muhammad Sadiq et al., Mater. Res. Express 8 095507(2021); https://doi.org/10.1088/2053-1591/ac2377

[8] Pia Dally Cellules Solaires à base de Matériaux Pérovskites : De la caractérisation des matériaux à l'amélioration des rendements et de la stabilité. Thesis November 2019, https://www.researchgate.net/publication/339774391.

[9] Amrit Kumar Mishra, R.K. Shukla, Materials. Today: Proceedings 49(321)(January 2021); https://doi.org/10.1016/j.matpr.2020.11.376

[10] Muhammad Aitezaz Hussain, Sobab Khan, Ahtasham Rahim, Azam Jan, Mudasar Rashid, International Journal of Engineering Works ISSN-p: 2521-2419 ISSN-e: 2409-2770 Vol. 7, Issue 02, PP. 109-115, February 2020; https://doi.org/10.34259/ijew.20.702109115

[11] Dita Puspita, Computational and Experimental Research in Materials and Renewable Energy (CERIMRE) Volume 2, Issue 2, page 56-63 eISSN : 2747-173X November 24, 2019; https://doi.org/10.19184/cerimre.v2i2.27366

[12] T. Minemoto, M. Murata, Curr. Appl Phys. 14 (11) 1428-1433(2014); https://doi.org/10.1016/j.cap.2014.08.002

[13] L. Sims, U. Hörmann, R. Hanfland, R. C. I. MacKenzie, F. R. Kogler, R. Steim P. Schilinsky, OrgElectron., 15 (2014) 2862-2867; https://doi.org/10.1016/j.orgel.2014.08.010

[14] S.Bensenouci, K Rahmou, A. Aissat, Journal of Ovonic Research Vol. 20, No. 2, March - April 2024, p. 163 – 175; https://doi.org/10.15251/JOR.2024.202.163

[15] Y. Gao, R. C. I. MacKenzie, Y. Liu, B. Xu, P. H. M. van Loosdrecht, W. Tian, Adv. Mater. Interfaces 2 (2015) 1400555; https://doi.org/10.1002/admi.201400555

[16] Y. Liu, R.C.I. MacKenzie, B. Xu, Y. Gao, M. Gimeno-Fabra, D. Grant, P. H. M. van Loosdrecht, T. Wenjing, J. Mater. Chem. C. 3 (2015) 12260-12266; https://doi.org/10.1039/C5TC02678D